Scientific Review Engineering and Environmental Sciences (2024), 33 (4), 401–418

Sci. Rev. Eng. Env. Sci. (2024), 33 (4) https://srees.sggw.edu.pl

ISSN 1732-9353 (suspended) eISSN 2543-7496 DOI 10.22630/srees.9956

Received: 10.09.2024
Accepted: 17.10.2024

Sergii SURKOV[1]
Volodymyr KRAVCHENKO[3]
Iryna KORDUBA[2]
Andrii GOLOVCHENKO[3]
Oleksandr BUTENKO[1]
Serhii TSYBYTOVSKYI[2]✉
Yuliia TRACH[4]

[1] Odesa Polytechnic National University, Institute of Distance and Correspondence Education, Ukraine
[2] Kyiv National University of Construction and Architecture, Department of Environmental Protection Technologies and Labor Protection, Ukraine
[3] Odesa Polytechnic National University, Nuclear Power Plants Department, Ukraine
[4] Warsaw University of Life Sciences – SGGW, Institute of Civil Engineering, Poland
National University of Water and Environmental Engineering, Institute of Agroecology and Land Management, Ukraine

Use of an ejector to reduce the time of air injection during testing of the containment system at nuclear power plants

Keywords: airtight enclosure system, air injection time, optimal ejector design

Introduction

The further development of nuclear energy is based on three main principles: safety, cost-effectiveness, and public attitude (Shirokov, 1997). All these principles are interrelated. To ensure safe operation, nuclear power plants (NPPs) are

✉serhii.uaror@gmail.com

Surkov, S., Kravchenko, V., Korduba, I., Golovchenko, A., Butenko, O., Tsybytovskyi, S., Trach, Y. (2024). Use of an ejector to reduce the time of air injection during testing of the containment system at nuclear power plants. *Sci. Rev. Eng. Env. Sci.*, *33* (4), 401–418. DOI 10.22630/srees.9956

equipped with the necessary safety systems that prevent accidents and are designed to keep equipment from being destroyed in the case of accidents. Localizing safety systems are designed to contain radioactive substances within the unit and prevent their release into the environment. Of course, the availability of safety systems affects both the cost and operational performance of a nuclear power plant.

In ensuring the required level of safety, the cost performance of power plants is crucial when deciding on the choice of an energy source. Therefore, nuclear power is always in competition with other energy sources; recently it was gas power plants while today it is renewable energy sources, as these already have specific capital investments at the level of nuclear power plants or less. However, today they are losing in terms of cost and unstable electricity production. It should be noted that the development of electricity storage solves the latter drawback and makes wind and solar power plants more popular, as they do not pose a nuclear threat. Thus, it should be emphasized that only the economic advantages of NPPs make them more acceptable in the market today.

Thus, during the NPP operation, great attention is paid to the safety systems that serve to maintain the integrity of the safety barriers. The latter are designed to prevent the release of radioactive fission products into the environment in the event of an accident. The containment system is the last system to prevent fission products from being released to the environment in the event of a severe accident. To confirm the readiness of this system to perform its functions in the event of an accident, appropriate leakage tests are performed after each repair.

The "absolute pressure" method is used to test the level of sealing of the containment system and elements of the accident localization system at Ukrainian NPPs. According to this method, the mass of air available in the CSA is determined by measuring the pressure, temperature and humidity according to the Mendeleev–Clapeyron equation. The tests consist of five stages: vacuuming; air injection to achieve the required pressure of 1.72 kg·cm^{-2}; stabilization of the parameters; measurement; and pressure release, as well as lasting more than 25 h. No work is carried out in the CSO during the tests. A compressor is used to provide the overpressure in the CSF and, given the large volume of the CSF, it takes a relatively long time to inject the air, which affects the economic performance of the NPP (Kravchenko et al., 2023).

Literature review and problem statement

In Kravchenko et al. (2022), it was proposed to use an ejector, the working medium for which is air after the compressor, to reduce the time of air injection. In this case, the ejector was calculated, its characteristic constructed, and the injection

time determined. A number of assumptions were made in the calculations, which is why the results were obtained with a corresponding error. It should be noted that equipment for cleaning the air of dust and moisture is installed directly after the compressor. Accordingly, when using the ejector, the air that is drawn into the ejector must also be cleaned of dust and moisture. The availability of this equipment was not considered on paper by Kravchenko et al. (2022). The presence of additional resistance at the inlet of the air drawn into the ejector should lead to a decrease in the air flow at the outlet of the ejector and an increase in the time of air injection to the required pressure in the CSO.

The aim of this study is to clarify the results obtained in a paper by Kravchenko et al. (2022), regarding minimizing the time for air injection into the CSU during leakage tests. To achieve this goal, the following tasks were performed:

- An algorithm for calculating the gas ejector was developed, adapted to the case when the full pressures in all nozzles are set.
- The dynamics of air injection into the CSO under variable pressure were then calculated and the injection time determined.
- The dynamics of air injection into the CSO under variable pressure were then calculated and the injection time determined.
- The design and operational factors that affect this time were determined.
- The ejector design was optimized with respect to the minimum air injection time.

Compressor operation without an ejector

Before starting the calculation of the ejector itself, it is necessary to build a characteristic for the gas compressor that injects the working air flow.

To solve this problem, the first step is to obtain the compressor characteristic in the form of the flow versus the backpressure at the outlet. In addition, it is advisable to immediately convert the volume flow rate to a mass flow rate, given that the 'normal cubic meters' are calculated at an air temperature of 0°C. In this case, the mass air supply is calculated as follows:

$$G = \rho Q = \frac{p_{\text{abc}} Q}{\text{RT}}, \tag{1}$$

where: G – mass air supply [kg·s^{-1}], ρ – air density [kg·m^{-3}], Q – volume flow rate [m^3·s^{-1}]; p_{abc} – absolute pressure (p = 101,325) [Pa], R – specific gas constant (R_{air} = 287) [J·kg^{-1}·K^{-1}], and T – absolute thermodynamic temperature (T = 273.15) [K].

Surkov, S., Kravchenko, V., Korduba, I., Golovchenko, A., Butenko, O., Tsybytovskyi, S., Trach, Y. (2024). Use of an ejector to reduce the time of air injection during testing of the containment system at nuclear power plants. *Sci. Rev. Eng. Env. Sci.*, *33* (4), 401–418. DOI 10.22630/srees.9956

Figure 1 shows the characteristic of the TsK-35/8 centrifugal compressor.

In the AB section, at an overpressure of $p \leq 4.73$ bar, it is convenient to approximate the characteristic by the linear dependence:

$$G = 3.44669 - 0.04554p, \tag{2}$$

where: G – mass flow rate [kg·s^{-1}], p – overpressure at the compressor outlet [bar].

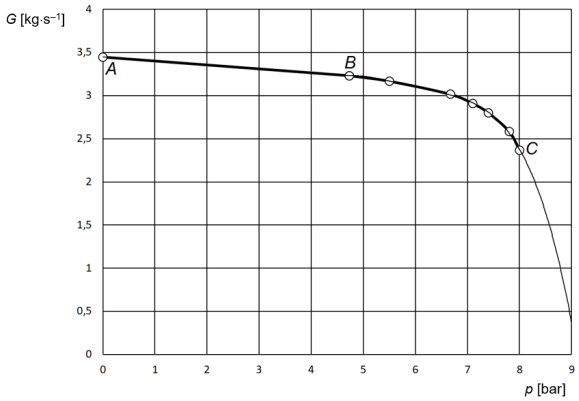

FIGURE 1. Approximation of the characteristics of the TsK-135/8 compressor
Source: own work.

In section BC, at an overpressure of $p > 4.73$ bar, a fourth-degree polynomial approximation is used:

$$G = -0.02774 \cdot p^4 + 0.6588 \cdot p^3 - 5.85566 \cdot p^2 + 22.94649 \cdot p - 30.13195.$$

This approximation provides a high value of the coefficient of agreement, $R^2 = 0.9987$. In addition, this approximation allows the characterization to be extended to the right of point C by extrapolation.

Since the overpressure in the CSO does not exceed 0.7 bar, the compressor characteristics in this range are described by a linear relationship. The fill time can then be determined analytically.

The differential equation describing the filling process can be represented as:

$$\frac{dm}{dt} = G(m), \tag{3}$$

where: m – mass of air inside the SGU [kg], $G(m)$ – mass flow rate of the air entering the SGU [kg·s^{-1}].

Hence:

$$dt = \frac{dm}{G(m)}. \tag{4}$$

This allows the calculation of certain integral:

$$t = \int_{m_1}^{m_2} \frac{dm}{G(m)}, \tag{5}$$

where: m_1 and m_2 – masses of air inside the containment at the beginning and end of the filling process.

The mass of air in the containment vessel is determined using a gas equation (Mendeleev–Clapeyron):

$$m = \frac{pv}{\mathrm{RT}}, \tag{6}$$

where: V – volume of air in the SGO [m^3].

We get m_1 = 72.260 kg and m_2 = 121.235 kg.

Absolute pressure is related to mass:

$$p_{\mathrm{abc}} = \frac{m\mathrm{RT}}{v}. \tag{7}$$

But the compressor characteristic (2) uses an overpressure expressed in bars. We can define it by the formula

$$p = \frac{p_{\mathrm{abc}} - 101{,}325}{100{,}000} = \frac{m\mathrm{RT}}{100{,}000 \cdot v} - 1.01325 \text{ [bar]}.$$

Then the dependence of the compressor supply on the mass of air in the CSO is described by the equation:

$$G(m) = 3.44669 - 0.045543\left(1.40223 \cdot 10^{-5} m - 1.01325\right) = 3.40054 - 6.38619 \cdot 10^{-7} m. \tag{8}$$

Surkov, S., Kravchenko, V., Korduba, I., Golovchenko, A., Butenko, O., Tsybytovskyi, S., Trach, Y. (2024). Use of an ejector to reduce the time of air injection during testing of the containment system at nuclear power plants. *Sci. Rev. Eng. Env. Sci.*, *33* (4), 401–418. DOI 10.22630/srees.9956

Integrating (5), we obtain the time for filling the CSO:

$$t = \int_{m_1}^{m_2} \frac{dm}{3.40054 - 6.38619 \cdot 10^{-7} m} = \frac{\ln\left(3.40054 - 6.38619 \cdot 10^{-7} m\right)}{-6.38619 \cdot 10^{-7}} \Big|_{m_1}^{m_2}. \quad (9)$$

The time is equal to 14,274 s or 3.965 h. The result obtained analytically is the same as the result of the numerical integration.

Calculation of a gas ejector (jet compressor)

Although gas ejectors have long been known and are widely used in various industries, research on ejectors continues. Their typical use is in the oil and gas industries (Carpenter, 2020; Ping & Macdonald, 2020; Bernat et al., 2023), and in the energy industry (Sammak et al., 2021).

A number of studies have been devoted to optimizing the geometry of ejectors. For this, 1D models (Wang et al., 2021; Van den Berghe et al., 2022) and 3D models are used (Butenko & Smyk, 2015; Shi et al., 2024), as well as neural networks (Gupta et al., 2021).

Further improvement of the ejectors is possible due to the use of pulse ejectors (Voropaiev et al., 2021), gas-wave ejectors (Li et al., 2024), and vortex separation ejectors (Novruzova & Qadashova, 2020).

The peculiarity of our calculation is that we need to minimize the time of increasing the air pressure in the CSA by means of the ejector, considering the fact that the pressure inside the CSA is continuously changing. This led to the need to change the sequence of calculations within the classical mathematical model of the ejector.

Figure 2 shows the design scheme of an ejector with a cylindrical mixing chamber. The figure shows the parameters of the working, ejected and mixed flow, as well as the main sections for which the equations are drawn up.

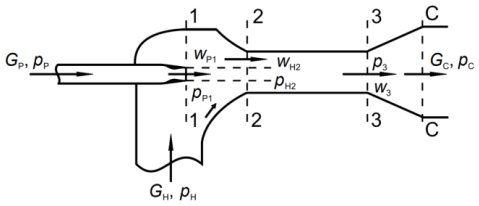

FIGURE 2. Design scheme of the gas ejector

Source: own work.

The equations describing the operation of the ejector include the continuity equations:

$$G_p + G_H = G_c. \tag{10}$$

As well as the equation of conservation of momentum of the quantity of motion:

$$\varphi_2 \left(G_p w_{p_2} + G_H w_{H_2} \right) - \left(G_p + G_H \right) w_3 = \left(p_3 + p_{p_2} \right) f_{p_2} + \left(p_3 + p_{H_2} \right) f_{H_2}, \tag{11}$$

where: φ_2 – velocity coefficient of the mixing chamber, w_i – gas velocities in the corresponding sections [m·s^{-1}], p_i – absolute gas pressures of gas velocities in the corresponding sections [Pa], and f_i – cross-sectional areas [m^2].

The usual assumption of pressure equality is used:

$$p_{p_2} = p_{p_1} = p_H. \tag{12}$$

The presence of energy losses in different parts of the ejector is considered using velocity coefficients. The following values of speed coefficients are recommended:
- working nozzle: $\varphi_1 = 0.95$,
- mixing chamber (MC): $\varphi_2 = 0.975$,
- diffuser: $\varphi_3 = 0.9$,
- inlet section of the CP: $\varphi_4 = 0.925$.

The peculiarity of supersonic gas ejector calculations is that they consider the compressibility of gases. In this case, the speed of the working flow usually exceeds the speed of sound. Traditionally, gas-dynamic functions are used in the calculated-reduced pressure:

$$\Pi(\lambda) = \left(1 - \frac{k-1}{k+1} \lambda^2 \right)^{\frac{k}{k-1}} \tag{13}$$

and reduced mass velocity

$$q(\lambda) = \left(\frac{k+1}{2} \right)^{\frac{k}{k-1}} \lambda \left(1 - \frac{k-1}{k+1} \lambda^2 \right)^{\frac{k}{k-1}}, \tag{14}$$

where: λ – reduced velocity, k – adiabatic index.

Surkov, S., Kravchenko, V., Korduba, I., Golovchenko, A., Butenko, O., Tsybytovskyi, S., Trach, Y. (2024). Use of an ejector to reduce the time of air injection during testing of the containment system at nuclear power plants. *Sci. Rev. Eng. Env. Sci.*, *33* (4), 401–418. DOI 10.22630/srees.9956

We assume that the main geometric parameter, the ejector module, is given:

$$M = \frac{f_3}{f_{p^*}}, \tag{15}$$

where: f_3 – cross-sectional area of the cylindrical mixing chamber [m^2], f_{p^*} – critical cross-sectional area of the working air nozzle [m^2].

The total pressure in all three nozzles is also given, and therefore the air compression ratio:

$$\varepsilon = \frac{p_c}{p_H}. \tag{16}$$

It is necessary to determine the air flow rate in all nozzles and the ejection coefficient: $u = \frac{G_H}{G_p}$.

Working flow

First of all, the parameters of the working flow can be calculated since it does not depend on the ejection ratio. The working air flow rate is set based on the compressor capacity.
The gas-dynamic function is calculated as follows:

$$\Pi_{p_2} = \frac{p_H}{p_p}. \tag{17}$$

Using (6), the reduced velocity can be determined analytically:

$$\lambda_{p_2} = \sqrt{\frac{k+1}{k-1}\left[1 - \Pi_{p_2}^{\frac{k-1}{k}}\right]}. \tag{18}$$

It should be borne in mind that the velocity at the outlet of the working nozzle is usually supercritical, i.e., $\lambda_{p_2} > 1$. The reduced mass velocity q_{p_2} is calculated using (18). Next, the outlet cross-sectional area of the nozzle is calculated:

$$f_{p_2} = \frac{f_{p^*}}{q_{p_2}}. \tag{19}$$

The cross-sectional area of the ejected flow is 2-2:

$$f_{H_2} = f_3 - f_{p_2} v. \tag{20}$$

Critical speed at a given air temperature:

$$a_* = \sqrt{\frac{2k}{k+1}}\mathrm{RT}. \tag{21}$$

Working fluid velocity at the nozzle outlet

$$w_{p_2} = \varphi_1 a_* \lambda_{p_2}. \tag{22}$$

In most literature, when calculating the ejector characteristics, the ejection coefficient u is set and the compression ratio ε is calculated. However, with this calculation sequence, it is difficult to determine the maximum value of the ejection coefficient, which significantly reduces the accuracy of calculating the filling time of the CSO.

In the course of the work, the calculation methodology was improved and it was proposed to set the compression ratio ε and calculate the ejection coefficient. In this case, the convergence of the results is significantly improved.

The calculation of the ejector characteristic is performed under the assumption that the air movement is adiabatic. In this case, the characteristic would have the form ABC (Fig. 3). It should be noted that on the ABC line, each value of the ejection coefficient corresponds to two values of the compression coefficient, which led to poor convergence of the iterative process using the Gauss–Seidel method.

It is known from experiments that when the speed of sound reaches Section 3-3, the so-called flow closure occurs. In this case, despite changes in pressure, the air velocity in the critical section remains constant and equal to the local speed of sound. This phenomenon corresponds to the vertical section BD in Figure 3, and the real characteristic of the ejector is ABD.

In addition, it is theoretically possible to close the flow in Sections 1-1 and 2-2, but these critical modes are not realized under the studied parameters.

Surkov, S., Kravchenko, V., Korduba, I., Golovchenko, A., Butenko, O., Tsybytovskyi, S., Trach, Y. (2024). Use of an ejector to reduce the time of air injection during testing of the containment system at nuclear power plants. *Sci. Rev. Eng. Env. Sci.*, *33* (4), 401–418. DOI 10.22630/srees.9956

Mixed flow

At each step, the value of λ_{c_3} is set in the range from 0 to 1. The condition λ_{c_3} ensures that the mixed flow velocity is subsonic.

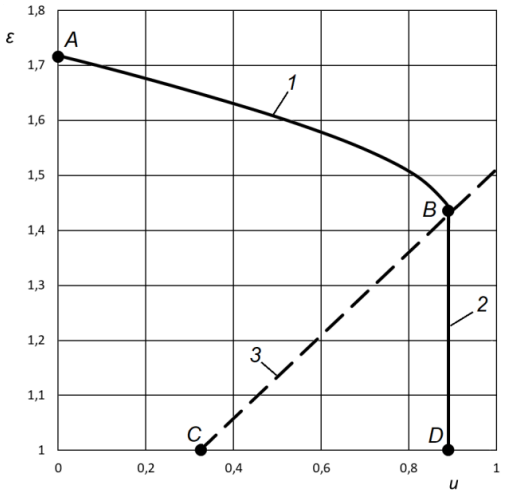

FIGURE 3. Calculated characteristic of the ejector at $M = 8.6$ (1 – adiabatic characteristic, 2 – short-circuit mode in Section 3-3, 3 – critical mode limit in Section 3-3)

Source: own work.

For a given value of λ_{c_3}, we determine the values of the gas-dynamic functions λ_{c_3} and q_{c_3} pressure at the outlet of the mixing chamber:

$$p_3 = \Pi_{c_3}. \tag{23}$$

Mixed flow velocity in Section 3-3 is calculated as follows:

$$w_3 = \frac{a_* \lambda_{c_3}}{\varphi_3}, \tag{24}$$

where: φ_3 – diffuser velocity coefficient.

Since the modulus of the ejector is given, we determine the cross-sectional area of the CS:

$$f_3 = M f_{p*} \tag{25}$$

and then the mixed flow rate:

$$G_c = \frac{k\Pi_* p_c q_{c_3} f_3}{a_*}. \tag{26}$$

Therefore, the flow is ejected.

From the mass conservation equation, we determine the mass flow rate:

$$G_H = G_c - G_p. \tag{27}$$

In the case of a cylindrical mixing chamber:

$$f_{H_2} = f_3 - f_{p_2}. \tag{28}$$

The reduced mass velocity of the ejected flow in Section 2-2:

$$q_{H_2} = \frac{G_H a_*}{k_H \Pi_{H*} p_H f_{H_2}}. \tag{29}$$

Knowing q_{H_2}, it is impossible to determine the reduced velocity λ_{H_2} analytically, so it is determined by the numerical method. After that, Π_{H_2} is determined.

Ejected flow velocity in Section 2-2 is calculated as follows:

$$w_{H_2} = \varphi_4 a_* \lambda_{H_2}, \tag{30}$$

Then the pressure of the ejected flow in Section 2-2:

$$p_{H_2} = \Pi_{H_2} p_H. \tag{31}$$

All the found values are substituted into the momentum balance equation (11) and the inviscidity is calculated, i.e., the difference in the total momentum from zero.

The subroutine for determining the root of a nonlinear algebraic equation automatically changes the value of λ_{c_3} in a given range until this inviscidity becomes zero with a given permissible error. Thus, at a given pressure p_c the value of λ_{c_3} is determined such that the law of mass conservation (5) and the law of momentum conservation (11) are fulfilled. After specifying λ_{c_3}, the ejection coefficient u can be determined. Figure 4 shows the dependence of the flow compression ratio ε as a function of the ejection coefficient *u* at three values of the ejector module.

Surkov, S., Kravchenko, V., Korduba, I., Golovchenko, A., Butenko, O., Tsybytovskyi, S., Trach, Y. (2024). Use of an ejector to reduce the time of air injection during testing of the containment system at nuclear power plants. *Sci. Rev. Eng. Env. Sci.*, *33* (4), 401–418. DOI 10.22630/srees.9956

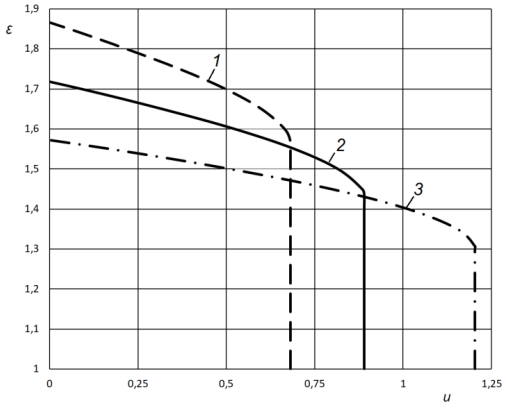

FIGURE 4. Dependence of the flow compression ratio ε to the ejection coefficient *u*
Source: own work.

Characteristics of ejectors at different modulus values:

$$1 - M = 7.0;\ 2 - M = 8.6;\ 3 - M = 11.0 \tag{32}$$

Figure 4 shows that ejectors that provide high ejection rates have a limited compression ratio. Our goal is to find an ejector module that provides an optimal balance between these indicators.

Based on the obtained characteristics, the next step is to model the dynamics of air injection into the CSO to determine the optimal ejector module.

Dynamics of the process of air injection into the CSU

The pressure in the CSA is related to the mass of the gas contained there, based on the equation of the state of gas or the Mendeleev–Clapeyron equation. The dependence of air mass on time is expressed by the differential equation (3). The calculation of the dynamics of filling the containment is reduced to the numerical solution of the differential equation (3). The solution was performed using the Runge–Kutta–Felberg method of the fourth order or fifth of accuracy with automatic selection of the integration step.

The dependence of the pressure in the zones on time at different ejector modules is shown in Figure 5.

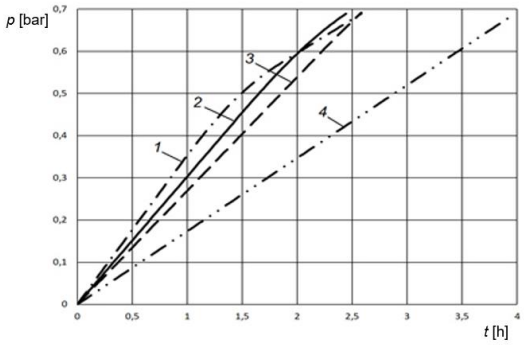

FIGURE 5. Dynamics of pressure change in the SG at different ejector modules (1 – M = 7.0; 2 – M = 8.6; 3 – M = 11.0; 4 – compressor without ejector)

Source: own work.

Curve 4 in Figure 5 shows the filling of the storage tank directly from the compressor without the use of an ejector. The figure shows that in this case, the filling time is maximum and is approximately 4 h. Curve 3 shows the dynamics of filling the storage tank with an ejector module of 7.0. The filling rate remains at the approximately constant, albeit low. Curve 1 corresponds to a module of 11.0. At the beginning the filling rate is high, but in the upper part of the graph the ejection ratio decreases, and in fact one compressor is working. Finally, Curve 2 corresponds to a modulus of 8.6, which ensures the shortest possible filling time.

Figure 6 shows the dependence of the charge time on the ejector module.

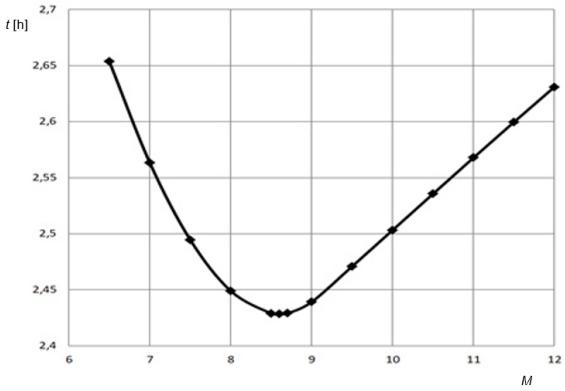

FIGURE 6. Dependence of the time of filling of the ZO on the ejector module

Source: own work.

Surkov, S., Kravchenko, V., Korduba, I., Golovchenko, A., Butenko, O., Tsybytovskyi, S., Trach, Y. (2024). Use of an ejector to reduce the time of air injection during testing of the containment system at nuclear power plants. *Sci. Rev. Eng. Env. Sci.*, *33* (4), 401–418. DOI 10.22630/srees.9956

Figure 6 shows that the shortest filling time is achieved with a module of 8.6 and is approximately 2.43 h. This means that the use of an ejector reduces the filling time by 38.8%.

Figure 7 shows the dependence of the filling time of the ash container on the overpressure in front of the working nozzle.

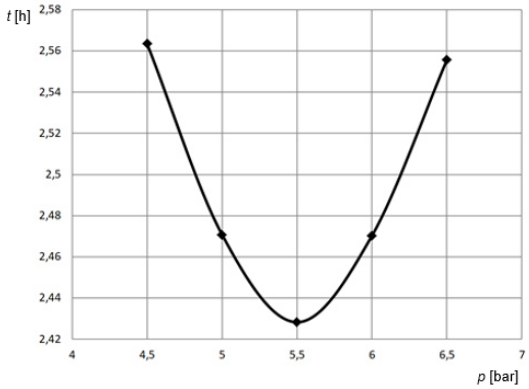

FIGURE 7. Dependence of the filling time of the nozzle on the pressure before the nozzle
Source: own work.

Figure 7 shows that the optimal overpressure is 5.5 bar. The fact is that at high compressor outlet pressures, the compressor flow rate decreases. In this case, despite the high ejection coefficients, the total flow rate at the ejector outlet decreases.

Effect of additional resistances

When calculating the air injection to the cooling zone, it is necessary to consider the effect of the air filters, which represent an additional hydraulic resistance.

The preliminary calculation uses the velocity coefficients φ, which are related to loss coefficients ζ by the ratio:

$$\zeta = \frac{1}{\varphi^2}. \tag{33}$$

The additional drag coefficient (ζ_D) affects the velocity coefficient as follows:

$$\varphi = \frac{1}{\sqrt{\zeta + \zeta_D}}. \tag{34}$$

There is currently no reliable information on the loss factor. The data sheet of the dust filter installed at the compressor outlet shows that its aerodynamic resistance is 0.1 bar. If we assume that the resistance of the moisture separator will be equal to 0.1 bar, then we note that the total resistance of the two filters that must be additionally installed at the inlet of the air drawn into the ejector will be equal to Δp = 0.2 bar with a filter nozzle diameter of D = 0.15 m. To determine the appropriate loss factor, we can perform the calculation under the conditions of installation directly behind the compressor.

– for volume flow to the compressor:

$$Q = \frac{G}{\rho} = \frac{3.4}{1.2} = 2.83 \text{ m} \cdot \text{s}^{-1}, \tag{35}$$

– for air velocity:

$$w = \frac{4Q}{\pi D^2} = \frac{4 \cdot 2.83}{\pi \cdot 0.15^2} = 160 \text{ m} \cdot \text{s}^{-1}, \tag{36}$$

– then the additional loss factor:

$$\zeta_D = \frac{2\Delta p}{\rho w^2} = \frac{2 \cdot 20{,}000}{1.2 \cdot 160^2} = 1.3. \tag{37}$$

According to Equation 34, we obtain φ_4 = 0.636. The calculated characteristic of the ejector with this value of the speed coefficient is shown in Figure 8.

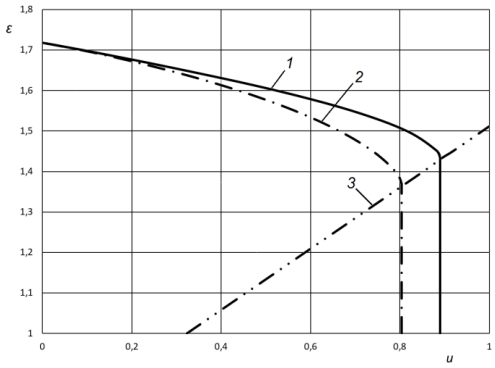

FIGURE 8. Effect of additional resistance on the ejector characteristic: 1 – φ_4 = 0.925 (standard settings), 2 – φ_4 = 0.636 (filter at the input), 3 – critical mode limit in Section 3-3

Source: own work.

The calculations of the dynamics of the process of filling the CSO show that, in the presence of additional resistances, the useful effect of the ejector decreases. When a filter is installed at the inlet of the suction flow, the estimated time for filling the CSG is 2.56 h. That is, the reduction in filling time due to the ejector is 35.5%.

Although the installation of the filter somewhat reduces the useful effect of using the ejector, the reduction in air injection time by 35.5% is significant. The installation of the ejector can be recommended for practical implementation.

Conclusions

In this work, we have developed an algorithm for calculating a gas ejector, which differs from the classical algorithm in the sequence of calculations and uses modern numerical methods. The modeling of the process of filling the gas ejector was performed by numerical solution of the differential equation. The air injection time is optimized by two parameters – the ejector module and the compressor outlet pressure.

The calculation shows that the ejector can reduce the time of filling the CSA by 38.8%, which will reduce the total test time.

The presence of a filter at the inlet of the ejected air reduces the effect of using the ejector: the reduction in discharge time will be equal to 35.5%.

Further theoretical and experimental studies are needed to clarify the results obtained.

References

Bernat, M., Nagy, S., & Smulski, R. (2023). Use of a New Gas Ejector for a TEG/TREG Natural Gas Dehydration System. *Energies*, *16* (13), 5011. https://doi.org/10.3390/en16135011

Butenko, O. G., & Smyk, S. Y. (2015). Improvement of the central ejector efficiency under nonoptimal operating modes. *Scientific Bulletin of National Mining University*, *2*, 57–61.

Carpenter, C. (2020). Installation of gas ejector provides boost to low-pressure gas well. *Journal of Petroleum Technology*, *72* (11), 69–70. https://doi.org/10.2118/1120-0069-JPT

Gupta, P., Kumar, P., & Rao, S. M. (2022). Artificial neural network model for single-phase real gas ejectors. *Applied Thermal Engineering*, *201* (Part A), 117615. https://doi.org/10.1016/j.applthermaleng.2021.117615

Kravchenko, V. P., Vlasov, A. P., Holovchenko, A. M., Mazurenko, A. S., Dubkovsky, V. O., & Chulkin, O. O. (2023). Status and prospects of testing the hermetic enclosure system of the reactor plant with VVER-1000 for tightness. *Nuclear and Radiation Safety*, *2* (98), 53–60.

Kravchenko, V., Vlasov, A., Andryuschenko, A., Vlasov, D., Golovchenko, A., & Gavrilov, P. (2022). Reduced air injection time during containment testing due to the use of an ejector. *Proceedings of Odessa Polytechnic University*, *1* (65), 62–69.

Li, H., Zhao, Y. & Hu, D. (2024). Simulation and analysis of pressure waves in flow channels of axial and radial gas wave ejectors. *Recent Patents on Engineering* (in press). http://dx.doi.org/10.2174/0118722121321712240724075604

Novruzova, S. G., & Qadashova, E. V. (2020). Possibility of vortex separation ejector application in the collection and separation of gas. *News of the Academy of Sciences of the Republic of Kazakhstan, Series of Geology and Technical Sciences*, *5* (443), 150–155. https://doi.org/10.32014/2020.2518-170X.115

Ping, W. & Macdonald, B. (2020, October 25). *Giving a boost to low pressure gas well by installing gas ejector* [Conference session]. SPE/IATMI Asia Pacific Oil & Gas Conference and Exhibition, Bali, Indonesia. https://doi.org/10.2118/196440-MS

Sammak, M., Ho, C., Dawood, A., & Khalidi, A. (2021). Improving combined cycle part load performance by using exhaust gas recirculation through an ejector. *Turbo Expo: Power for Land, Sea, and Air*, *84966*, V004T06A012. https://doi.org/10.1115/GT2021-59358

Shi, H., Wang, R., Xiao, Y., Zhu, X., Zheng, R., Song, C., & Liu, Z. (2024). Optimization of exhaust ejector with lobed nozzle for marine gas turbine. *Brodogradnja*, *75* (3), 75303. http://dx.doi.org/10.21278/brod75303

Shirokov, S. V. (1997). *Yadernyye energeticheskiye reaktory* [*Nuclear power reactors*]. KPI.

Van den Berghe, J., Dias, B. R., Bartosiewicz, Y., & Mendez, M. A. (2023). A 1D model for the unsteady gas dynamics of ejectors. *Energy*, *267*, 126551. https://doi.org/10.1016/j.energy.2022.126551

Voropaiev, G. O., Zagumennyi, I. V., & Rozumnyuk, N. V. (2021). Modeling of gas – dynamic processes in the elements of impulse ejector. *Journal of Numerical and Applied Mathematics*, *1* (135), 66–72. https://doi.org/10.17721/2706-9699.2021.1.08

Wang, Z., Wang, S., Li, Y., Chen, L., & Zhang, H. (2021). Design and numerical investigation of ejector for gas pressurization. *Asia-Pacific Journal of Chemical Engineering*, *16* (3), e2625. https://doi.org/10.1002/apj.2625

Summary

Use of an ejector to reduce the time of air injection during testing of the containment system at nuclear power plants. The containment system (CS) is the last barrier to the release of radioactive substances into the environment in the event of a nuclear accident. After each overload, this system is tested for its ability to perform its functions by determining the integral leakage, which should not exceed a certain value. The tests are

Surkov, S., Kravchenko, V., Korduba, I., Golovchenko, A., Butenko, O., Tsybytovskyi, S., Trach, Y. (2024). Use of an ejector to reduce the time of air injection during testing of the containment system at nuclear power plants. *Sci. Rev. Eng. Env. Sci.*, *33* (4), 401–418. DOI 10.22630/srees.9956

performed at an overpressure in the CS of 0.72 kg·cm^{-2}, which is achieved by injecting air with a compressor. The paper considers the use of an ejector to accelerate the injection process, which has a positive effect on the technical and economic performance of a nuclear power plant (NPP) power unit by increasing the amount of electricity generated, which is very important today, when the NPPs provide the maximum share of electricity generated in the country. Previous studies have evaluated the use of an ejector for this purpose, but they did not consider the need to install filters on the intake air stream. In addition, they used numerical methods that generate an error. The present work uses a mathematical apparatus that provides a more accurate result. The obtained calculated compressor injection time coincides with the actual injection time for the Rivne NPP power units. The design of the ejector ensures the minimum injection time is determined. The optimal ejector module is equal to 8.6 (the ratio of the cross-sectional area of the cylindrical mixing chamber to the critical cross-sectional area of the working air nozzle). This reduces the injection time by 38.8%. The suction air must be free of dust and moisture. Suitable filters have a total aerodynamic resistance of 0.2 bar. Taking these air filters into account slightly reduces the efficiency of the ejector. The final time of air injection using the ejector is 2.56 h, which reduces the time of air injection for testing by 35.5%.